

## Modeling a Tomato Dehydration Process Using Geothermal Energy

M. Kostoglou<sup>1</sup>, N. Chrysafis<sup>2</sup> and N. Andritsos<sup>2</sup>

<sup>1</sup> Chemistry Department, Aristotle University of Thessaloniki, Box 116, 541 24 Thessaloniki, Greece

<sup>2</sup>Department of Mechanical Engineering, University of Thessaly, Pedion Areos, 383 34, Volos, Greece

kostoglu@chem.auth.gr, nandrits@mie.uth.gr

**Keywords:** Industrial use, vegetable drying, modeling

### ABSTRACT

A tomato dehydration unit has been operating since 2001 in N. Erasmio, 25 km south of the city of Xanthi (Thrace), and produces “sun-dried” tomatoes. The unit uses low-cost geothermal water to heat atmospheric air to 55-58°C through finned-tube air heater coils. This work deals with the modeling of a tomato drying process in a semi-continuous tunnel drier using low-enthalpy geothermal energy. The modeling procedure consists of two stages: The first stage refers to the modeling of a single tomato piece, whereas the second stage is concerned with the modeling of the procedure of air drying of tomatoes by moving the trays in a tunnel at batches. The model can be used for the design and optimization of the continuous drying process existing in N. Erasmio and elsewhere.

### 1. INTRODUCTION

Dehydration (or drying) of foods is defined as the application of heat under controlled conditions aiming at removing the majority of the water normally present in a food by evaporation (Fellows, 2000). Dehydration of foods is one of the oldest methods used to improve food stability, i.e. to extend the shelf life of foods by a reduction in water activity. The drying process involves the slow removal of the largest part of water contained in the fruit or vegetable so that the moisture contents of the dried product is below 20%. In the Mediterranean countries the traditional technique of vegetable and fruit drying (including tomatoes) is by using the sun, a technique that has remained largely unchanged from ancient times. However, on an industrial scale, most fruit is dried under the sun, while most vegetables are dried using continuous forced-air processes.

Dried fruits and vegetables can be produced by a plethora of drying methods. The selection of the proper technique depends upon the type of food and the type of characteristics of the final product (e.g. Mujumdar, 1987). Tunnel-type driers are the most flexible and efficient dehydration systems and they are widely used in drying fruits and vegetables. In general, the whole drying process can be divided in three stages: (1) pretreatment stage (selecting, sorting, washing of fresh produce, processing for color preservation etc.), (2) drying stage (mainly using a hot air environment) and (3) post-drying treatment stage (quality control of the product, storage, packaging).

It has been demonstrated that low-medium temperature geothermal energy can be used efficiently in drying several temperature-sensitive fruits and vegetables. The scope of this paper is to model the process of tomato drying in a tunnel-type drier operating in a semi-continuous way. As it will be discussed below, this process using low-temperature

geothermal waters has been efficiently applied in our country in the past decade.

### 2. GEOTHERMAL DRYING

Dehydration-drying of agricultural products comprises an interesting application of low and medium-enthalpy geothermal energy, especially when dealing with sensitive fruits and vegetables. Fresh or recycled air is forced to pass through an air-water converter and to be heated to temperatures in the range 40-100°C. The hot air passes through or above trays or belts with the raw produce, resulting in the reduction on their moisture content. In geothermal drying, electric power is only used to drive fans and pumps. Based on 2005 statistics, “geothermal” drying of fruits, vegetable and other agricultural products is performed in 15 countries worldwide (Lund et al, 2005). The share of drying of agricultural products in the total energy use of direct geothermal applications was 0,8%, and the total energy use in 2005 exceeded  $270 \times 10^3$  TJ/year. The largest drying plants are located in New Zealand (drying of alfalfa, wood and paper pulp).

The first tomato dehydration unit worldwide has been operating since 2001 in the geothermal field of N. Erasmio, located 25 km south-west of Xanthi (Thrace). The unit uses low-salinity geothermal water (with a temperature of 60°C) to heat atmospheric air to 55-57°C in finned tube air heater coils. In fact, the plant uses the same geothermal well that during winter provides geothermal water for soil heating aiming at off-season asparagus cultivation and for heating of a 0.4-ha vegetable greenhouse. The hot air passes once-through above trays with fresh tomatoes placed in the drying tunnels. The dehydration plant covers an area of about 400 m<sup>2</sup> housing two tunnel-type driers, washers, grading, cutting and packing equipment, offices and two storage rooms kept at a temperature less than 10°C. The length of each tunnel is 13.5 m, the height 2.2 m and the width 1.24 m. More information on the whole process can be found in Andritsos et al. (2003) and a schematic of one tunnel drier is depicted in Figure 1.

The amount of time required to dry tomatoes depend upon the tomato variety, the temperature and humidity of incoming hot air, the air velocity, the thickness of the tomato slices and the efficiency of the drier. The residence time of the product (for tomatoes of roma variety) in the drier is about 32 hours, fixed after a trial-and-error procedure. The raw produce (mainly well but not over-ripened tomatoes of the roma variety) is grown locally. The final “sun-dried” product is usually sold as a delicatessen food at an added value. The solids content of tomatoes used in the units ranges between 8 to 10% w/w and the moisture content of the final product is estimated to be less than 20%. Accordingly, the weight of the processed product is reduced about 10-12 times after drying. Currently the plant

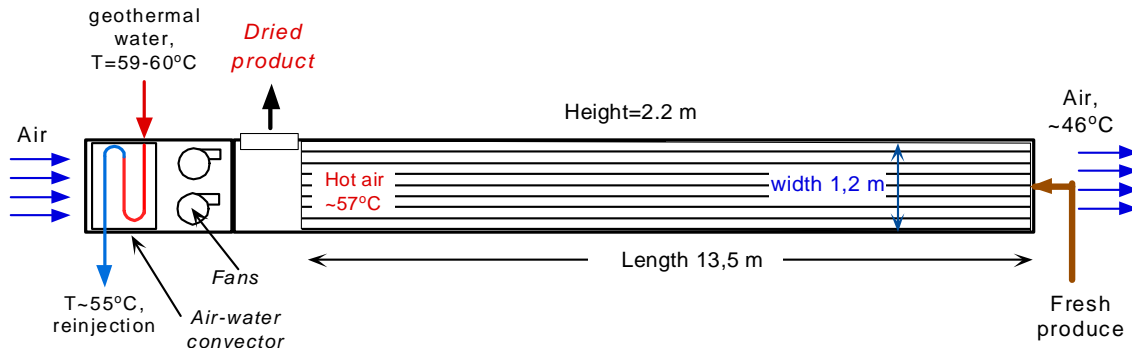


Figure 1: Schematic of the tunnel drier for tomato dehydration.

is capable of producing more than 1000 kg per day of dehydrated tomatoes with 10% moisture from 10-12 tn of fresh produce. The final product is stored in conditioned storage rooms. During the first eight years of operation of the dehydration plant 68 tn of high-quality dried tomatoes were produced, sold in Greece and abroad. The annual evolution of dried tomato production is illustrated in Figure 2. The unit is capable of drying and other vegetables and fruits and indeed, more than 1500 kg of peppers, figs, aubergines, cherries and apples have been also dried upon demand in the past three years.

the tunnel at batches. For the first stage the problem is rather to select than to develop a particular model since there is a plethora of drying models for food-stuff in the literature from quite empirical to relatively fundamental ones, each one covering particular aspects of the process. The second stage requires the development of a model based on the appropriate mass and heat balances valid under reasonable assumptions. This is a new development since the particular drying operation has not been studied in the literature according to our knowledge.

### 3.1 Stage I. Single Tomato Drying Model

Foods are extremely complex in their structure so there is not a general acceptable way to model their drying behavior leading to the appearance in the literature of several modeling methodologies. The most usual are the lumped purely empirical models resulting by simply fitting the drying curves and offering no other type of information (e.g. Mujumdar, 1987; Togrul, 2005). Nevertheless sometimes it is attempted to relate the fitting parameters with parameter having a physical meaning like the diffusion coefficient (Keey, 1972). Regarding the more phenomenological approaches their use depends on the nature of the product undergoing drying. The two major categories of the products are the porous and the non-porous. The actual mechanisms of drying for the two categories are different; capillarity dominates in the first case and molecular diffusion in the second case. Nevertheless, models developed for the one category are used for the other very usual in the literature. Even in reality, materials being nonporous at the beginning of drying, are transformed to porous at the later stages (e.g. Vallous et al, 2002).

Let us have a look at the possible modeling approaches for the case of porous materials. The most fundamental approach is the direct solution of the governing equations (using advanced techniques as the Lattice-Boltzmann methods in a geometry similar to this of the material (reconstructed from two dimensional images or X-ray tomography). Although this approach is feasible today, its value for engineering type calculations is questionable. The next level of reduced sophistication is to use instead of the actual geometry of the material, a network of pores with idealized shape (Yiotis et al, 2006). The literature is rich in models of this level but although they are useful to analyze the interaction between the scales (pore vs macroscopic) their value for engineering calculations is also questionable. At the next level the geometry is greatly simplified and the material is considered as homogeneous

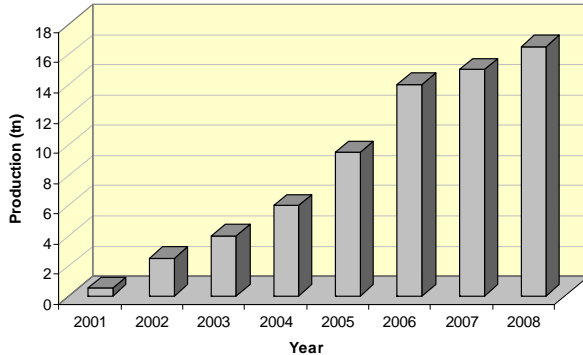


Figure 2: Annual production of “sun-dried” tomatoes in metric tons.

It is by coincidence that the temperature of incoming air stream is 56-58°C, which is considered to be the optimum temperature for properly drying tomatoes that keep their dark red color and flavor. It is well known that at temperatures 80°C or higher, tomatoes to be dried harden on the outside and severe oxidative damage is taken place.

In a tunnel drier of the type used in N. Erasmio there are N trays with tomatoes along the direction of air flow. Every time period  $\delta t$ , the trays are moved by one position and the final tray with the dried product is removed and a new tray with fresh produce is introduced in the tunnel. The locations of the trays along the tunnel are given by the subscript  $i$  ( $i=1,2,\dots,N$ ).

### 3. MODELING OF THE DRYING PROCESS

The modeling procedure consists of two stages: The first is the modeling of the single tomato piece and the second is the modeling of the particular procedure for air drying of the tomatoes by moving the trays with the produce within

whereas the localized governing equations are transformed to effective ones valid for the assumed homogeneous materials. Three different approaches are met in the literature for the equations that describes the heat and mass transfer in the material undergoing drying (Kocaeef et al, 2007): i) At first the older one for the case of capillary porous media, the model of drying of Luikov (1975). This model includes coupled heat and mass transfer equations. ii) The second and simpler model is based on simple diffusion and conduction equations coupled to each other only through the boundary conditions. This model is actually valid only for non-porous materials but in drying literature, it is used for porous material too. An extended discussion on this inconsistency and on the exact relation of this model to the other homogeneous material models (i) and (iii) can be found in Datta (2006) (iii) The third and most complicated approach is the so called multiphase model which includes coupled equations for the heat, mass and momentum transfer. This model although more sophisticated than the others has the disadvantage that it contains a large number of phenomenological parameters.

Regarding the non-porous materials the only drying modeling approach includes the diffusion and conduction equations with boundary coupling. The shrinkage also is very important (more for non-porous and less for porous materials) and it is taken into account using from very sophisticated to empirical approaches.

Now having the above general view on what type of drying models exists in the literature let us examine the specific case of the tomato. Tomato (*solanum lycopersicum*) is a non-porous material with a very inhomogeneous structure. There are regions with quite different properties, obviously the drying of the internal more wet material is much easier than the material close to the surface of the tomato. Also the degree of shrinkage is extremely large. Despite all this complexity the experimental drying curves are very simple and can be fitted with a first order model (e.g. Kiranoudis et al, 1993) or equivalently a simple diffusion model (Krokida et al, 2003). The shape of the tomato piece considered in the present work is hemispherical but it is not appropriate to solve the diffusion equation in spherical coordinates since the evaporation of water occurs mainly from the plane surface. It is more relevant to approximate the semispherical piece with a cylindrical slice (with evaporation only from the upper side) of the same radius and of thickness resulting from the total mass conservation. In the case of tomato with a radius  $R$ , the equivalent slice thickness,  $d$ , can be derived by equating the volume of hemisphere to that of a cylindrical slice as

$$d = \frac{2R}{3} \quad (1)$$

Normally the diffusion model requires also the solution of the conduction equation in the material but as the drying time is very large with respect to the characteristic time for conduction in the tomato, transients can be ignored and it can be considered that the tomato has always a uniform temperature equal to this of the gas. Regarding shrinkage, it is not taken explicitly into account but it is considered that the drying acceleration resulting from the size reduction counterbalances the deceleration due to the reduction of the diffusivity as the water content decreases. So the overall process can be modeled as constant thickness-constant diffusivity, diffusion process. The governing equation (which is one-dimensional due to the geometry transformation described above) is:

$$\frac{\partial X}{\partial t} = D \frac{\partial^2 X}{\partial x^2} \quad (2)$$

where  $x$  is the vertical distance ( $x=0$  on the tray surface),  $t$  is the time and  $X$  the tomato moisture in dry basis and  $D$  is the effective diffusivity. One of the boundary conditions is the no-water flux on the tray surface (i.e.  $\left(\frac{\partial X}{\partial x}\right)_{x=0} = 0$ ).

The second boundary condition should be the regular convection condition for mass transfer from gas to solid. The mass transfer coefficient is well-known to depend on temperature. This more "fundamental" approach is abandoned here by introducing another aspect of empiricism. A Dirichlet boundary condition is assumed by setting the surface moisture equal to equilibrium moisture  $X_e$  for the particular conditions of the gas (temperature  $T_g$  and humidity  $X_g$ ) and the anticipated effect of the gas velocity on the overall drying rate is assigned to the (gas velocity dependent) diffusivity. So the second boundary condition takes the form  $X(d,t) = X_e(T_g, X_g)$ .

The next step is to solve the equation (2) with its boundary conditions. The problem can be solved analytically resulting in a series solution, but usually only the first term of the series (valid at large time) is taken into account. The analytical solution cannot be used for cases of non-constant gas conditions, so in order to avoid a numerical solution (inconsistent with the level of sophistication of the model), the following approximate solution technique is proposed: The moisture profile is assumed to have a parabolic shape (very similar to the sinusoidal profile of the first term of the analytical solution). The profile shape which fulfills both the boundary conditions is:

$$X = X_e + c(d^2 - x^2) \quad (3)$$

Taking the integral of the equation from  $x=0$  to  $x=d$  results in:

$$\begin{aligned} \int_0^d \frac{\partial X}{\partial t} dx &= \int_0^d D \frac{\partial^2 X}{\partial x^2} dx \Rightarrow \\ \frac{d}{dt} \int_0^d X dx &= D \left( \frac{\partial X}{\partial x} \right)_{x=d} - D \left( \frac{\partial X}{\partial x} \right)_{x=0} \end{aligned} \quad (4)$$

The average moisture in the tomato will be:

$$X_m = \frac{1}{d} \int_0^d X dx = X_e + \frac{2}{3} cd^2 \quad (5)$$

Now solving equation (3) with respect to  $c$  and substituting in (5) the moisture profile can be derived in terms of the average moisture. A further substitution in (4) leads to:

$$\frac{dX_m}{dt} = 3 \frac{D}{d^2} (X_m - X_e) \quad (6)$$

This equation is equivalent to the first term of the analytical solution but it has a slightly different proportionality coefficient. The present result is more appropriate in that it comprises a uniform approximation to the exact solution rather than a limiting case. The approach used here is similar to the so-called Linear Driving Force approximation which has been used extensively in adsorption studies and originally proposed by Glueckauf and Coates (1947).

Equation (6) is the final equation for the single tomato moisture evolution based on a compromise between fundamental mechanisms, literature and experience on one hand and simplicity, flexibility and parametric dependence on the other. According to this equation the gas state influences the drying process as follows: gas velocity influences the kinetics of the process ( $D$ ), gas humidity influences the driving force (equilibrium  $X_e$ ) and gas temperature influences both kinetics and equilibrium.

### 3.2 Stage 2: Drying Process Model

The drying process is shown schematically in Figure 1. The gas has an inlet temperature,  $T_{go}$ , an inlet humidity,  $X_{go}$  (kg water/kg air), and a mass flow rate  $F$ . The temperature and the humidity of the gas changes along the drying chamber and this is why a process model has to be developed in addition to the single tomato model. In the chamber there are  $N$  trays with tomatoes along the flow. At each time step  $\delta t$  the line with the trays proceeds by one tray position so the tomatoes of the final tray are received as dried product as one new tray is added to the line. The whole process operates in a periodic steady state but before trying to analyze its dynamics let us derive the governing equations ignoring the motion of the trays. The positions of the trays along the flow are denoted with the subscript  $i$  ( $i=1,2,\dots,N$ ). It is assumed that the conditions on each tray are uniform i.e. all the tomatoes on it drying at the same rate. This implies that the gas has constant properties over each tray. The region over a tray can be considered as a perfect gas mixture. This assumption is valid when the changes over the tray are not very pronounced and it corresponds to a finite volume discretization of the gas phase equations.

The evolution of the average moisture in tray  $i$  is given by:

$$\frac{dX_i}{dt} = \frac{3D_i}{d^2} (X_i - X_{ei}) \quad i=1,2,3,\dots,N \quad (7)$$

where  $X_{ei}$  is the equilibrium moisture corresponding to the local gas conditions ( $X_{gi}$ ,  $T_{gi}$ ) and  $D_i$  is the diffusivity corresponding to  $T_{gi}$ . The gas humidity balance over the tray  $i$  is (assuming perfect mixing):

$$F(X_{g+1} - X_{gi}) = m_i \frac{dX_i}{dt} \quad (8)$$

where  $m_i$  is the mass of tomato on tray  $i$ .

There is no need for an equation for the tomato temperature since, as it has been described in the previous section, tomato for the slow gas temperature variation in this situation is in thermal equilibrium with the gas. Consequently, it can be assumed that it always has the local gas temperature. A global heat balance in the gas phase for the tray  $i$  can be written as

$$Fc_p(T_{g+1} - T_{gi}) = m_i \Delta H \frac{dX_i}{dt} \quad (9)$$

The boundary conditions of the above problem are  $X_{g1}=X_{go}$ =inlet gas humidity and  $T_{g1}=T_{go}$ =inlet gas temperature. In case of batch operation of the process the initial condition is simply  $X_i=X_o$ =initial moisture of the tomato. For the case of periodic semi-continuous operation the situation is more complex. At a specific location  $i$  there is a periodicity of the tomato and gas properties associated to a period  $\delta t$ . Each tray has a residence time  $N\delta t$  and its motion along the tunnel is described in the Eulerian frame

of reference employed here, by the following conditions ( $j=1,2,\dots,N$ ):

$$\begin{aligned} \text{at } t = j\delta t: X_{i+1} &= X_i, X_f = X_N \\ (i &= 0,1,2,\dots,N-1) \end{aligned} \quad (10)$$

where  $X_f$  is the moisture of the final product. To better analyze the situation the following non-dimensional parameters are introduced:

$$\begin{aligned} D_o &= D(T_{go}); D_T = D(T_g) / D(T_{go}); \\ \tau &= 3D_o t / d^2; B = 3D_o m / (d^2 F); \\ p &= 3D_o \delta t / d^2 \end{aligned} \quad (11)$$

Using this dimensionless variables and some algebra the system of equations takes the form

$$\frac{dX_i}{d\tau} = (X_i - X_{ei}) \quad (12)$$

$$X_{gi+1} - X_{gi} = BD_{Ti}(X_i - X_{ei}) \quad (13)$$

$$T_{gi+1} - T_{gi} = BD_{Ti}(X_i - X_{ei}) \frac{\Delta H}{c_p} \quad (14)$$

As it can be seen in the above equations the key design parameters of the process are the number of trays  $N$ , the dimensionless time step  $p$  and the dimensionless parameter  $B$ . Fortunately, the mathematical problem has an analytical solution described by the following set of equations. For the time period between  $j\delta\tau$  and  $(j+1)\delta\tau$  it holds ( $j=0,1,2,\dots,N-1$ ):

$$\tau = jp + \tau' \quad (15a)$$

$$X_{j+1} = X_{ej+1} + (X_{jf} - X_{ej+1}) e^{-\tau'} \quad (15b)$$

$$X_{jf} = X_{ej} + (X_{j-1f} - X_{ej}) e^{-p} \quad (15c)$$

$$X_{gi+1} = BD_{Tj}(X_j - X_{ej}) + X_{gi} \quad (15d)$$

$$T_{gi+1} = BD_{Tj}(X_j - X_{ej}) \frac{\Delta H}{c_p} + T_{gi} \quad (15e)$$

In the above equations  $X_{jf}$  stands for the moisture of the tray  $j$  at time  $\tau=jp$  and  $X_{-1f}=X_o$ . The above relations give by sequential substitutions the temporal and spatial evolution of the variables  $X$ ,  $X_g$  and  $T_g$ . The solution is of Lagrangian type since index  $j$  refers to both the position along the dryer and time. To test the implementation of the above solution to a special algorithm some indicative results revealing the influence of the design parameters  $p$  and  $B$  on the drying process will be presented. A typical set of drying conditions is considered ( $X_o=9$ ,  $X_{go}=0.02$ ,  $T_{go}=60^\circ\text{C}$ ,  $N=25$ ,  $p=0.25$ ). The effect of the parameter  $B$  on the drying performance is shown in Figure 3. The curves in this figure can be interpreted in two ways: (i) as regular drying curves for the material of a particular tray as it moves along the dryer (Lagrangian description, time axis  $t/p$  with  $t=0$  being the moment the tray enters the dryer) and (ii) as spatial distribution along the dryer (Eulerian description, length axis  $z/L$  where  $L$  is the length that corresponds to a tray) at the time moment being an integer multiple of  $p$  (moment of changing tray position).

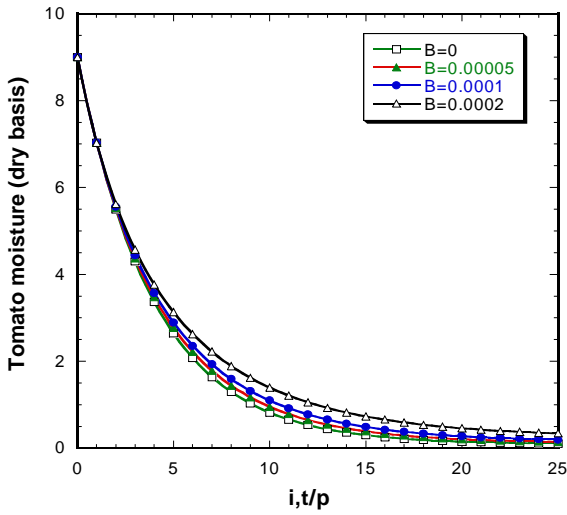


**Figure 3: Moisture profile of the product along the drier for various values of parameter B.**

When  $B=0$  the gas flow rate is large enough to keep the gas properties constant along the dryer. As  $B$  increases the gas humidity increases and its temperature decreases along the dryer leading to an increase of equilibrium moisture of the tomato and thus, to a reduced driving force for drying. This behaviour is shown in Figure 3. Also it can be noticed from this Figure that the largest amount of moisture removal is achieved at the first half of the residence time. Although this is true for all drying processes, it is more pronounced in the present dryer due to the variation of the gas properties along the flow (as time proceeds the drying driving force decreases).

The variation of the gas humidity along the dryer for several values of  $B$  is shown in Figure 4. As  $B$  increases the variation of gas humidity increases too. On the other hand, the temperature of the gas decreases along the dryer by an amount of cooling increasing with the value of  $B$  as it can be seen in Figure 5. From Figures 4 and 5 it is obvious that the most abrupt changes of the gas properties occur close to the entrance of the dryer.

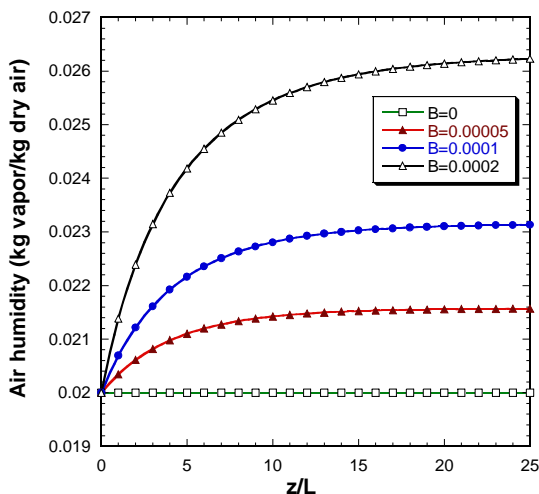


**Figure 4: Variation of gas humidity along the dryer for several values of B.**

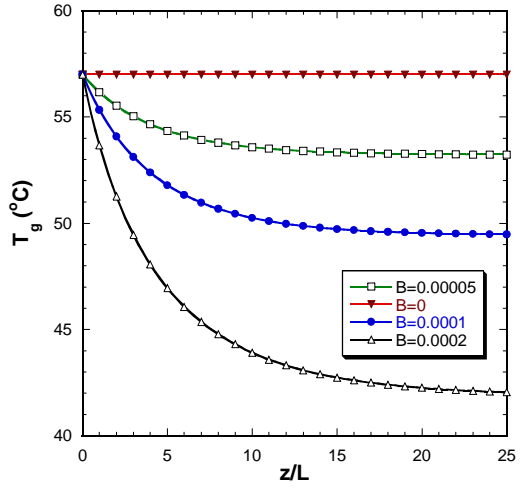


**Figure 5: Variation of gas temperature along the dryer for several values of B.**

The moisture of the dried product is presented against the value of  $B$  in Figure 6 for two values of the parameter  $p$ . As it is expected the moisture of the product increases as  $B$  increases and  $p$  (equivalent to drying time) decreases. Using a figure like this one, one can choose the appropriate drying time for a particular pair of desired product moisture and  $B$ .

The equilibrium moisture  $X_e$  is computed using the GAB equation which is the most widely used for foodstuffs and gives acceptable predictions in any case (e.g. Kiranoudis et al, 1996):

$$X_e = X_m C k \alpha_w [(1 - k \alpha_w)(1 - (1 - C)k \alpha_w)] \quad (16)$$

where  $X_m$  is the monolayer moisture content,  $\alpha_w$  the water activity, and  $C$ ,  $k$  are constants with an Arrhenius temperature dependency. The corresponding preexponential factors and activation energies, and also  $X_m$  can be found tabulated in the literature for several vegetables (with tomato among them). The water activity in the tomato is estimated as  $\alpha_w = RH/100$  where  $RH$  is the relative humidity of the air.

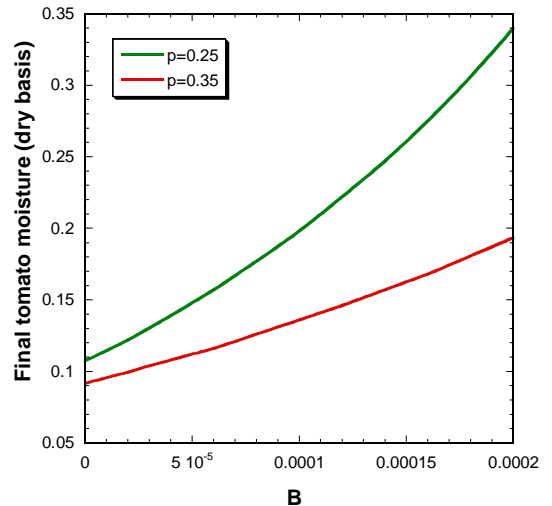


**Figure 6: Moisture of the final dried product for two values of the parameter  $p$ .**

The functional form with respect to gas velocity and temperature of the effective moisture diffusivity in the tomato is taken by Hawlander et al. (1991):

$$D = D_0 e^{1.022u^{0.5}} e^{-3024/T_g} \quad (17)$$

where  $u$  is the gas velocity. In the above general parametric study, the parameters were dimensionless so there was no need to know the value of  $D_0$ . In order to simulate an actual dryer and to give the results in dimensional units we have to estimate this value. This was done by simulating the batch experiments described in (Krokida et al, 2003) and requiring to find a similar drying time. The final result is  $D_0=2.3 \times 10^{-5} \text{ m}^2/\text{s}$ .

A particular continuous dryer will be simulated now. The total flow rate is  $28000 \text{ m}^3/\text{hr}$ , the vapor molar fraction in the inlet flow is 4% (corresponding to a relative humidity of 22%) and the inlet flow temperature is  $58^\circ\text{C}$ . There are 32 lines of trays with each line containing  $N=25$  trays. The time step  $\delta t$  equals to one hour. The spacing between the lines of trays is such that the gas velocity takes the value 1.5 m/s. The main parameter of which the effect will be studied here is the tomato loading of the tray ( $m$  in kg of tomatoes).

The drying curve for a particular tray (or equivalently the moisture distribution along the dryer) is shown in Figure 7 for several values of the tray loading  $m$ . In the limit of zero loading the final moisture is 10% but for loadings of practical interest the moisture of the product is much larger and increases with the loading. The only way to keep the product moisture low increasing the production rate  $m$  is to increase the air flow rate (in order to keep constant the value of parameter B).

The reason for the increase of the product moisture as  $m$  increases can become evident by observing Figures 8 and 9. In Figure 8 the gas humidity along the dryer for three values of  $m$  is presented. As  $m$  increases the humidity goes to larger values with the major increase to occur at the first stages of the dryer. On the opposite, as  $m$  increases the temperature goes to lower values. So the reason for large moisture of the product as  $m$  increase is not that the limited drying time but the shifting of the equilibrium due to the increased humidity and decreased temperature of the gas.

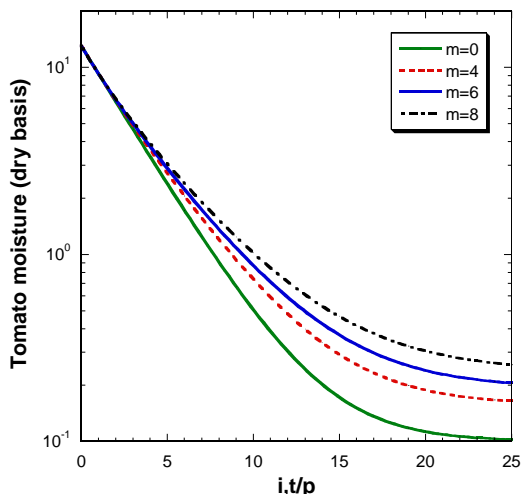


Figure 7: Moisture distribution along the drier for various tray loadings (kg/tray).

The moisture of the product is presented against the tray loading  $m$  in Figure 10 for several gas velocities (constant flow rate). Increasing the velocity from 1.5 m/s to 2 m/s has just a small influence on the product, definitely smaller than increasing flow rate with constant velocity. The model developed here after being calibrated with experimental results for a particular product (i.e. to find  $D_0$ ) can be used for the design and optimization of the continuous drying process studying in the present work.

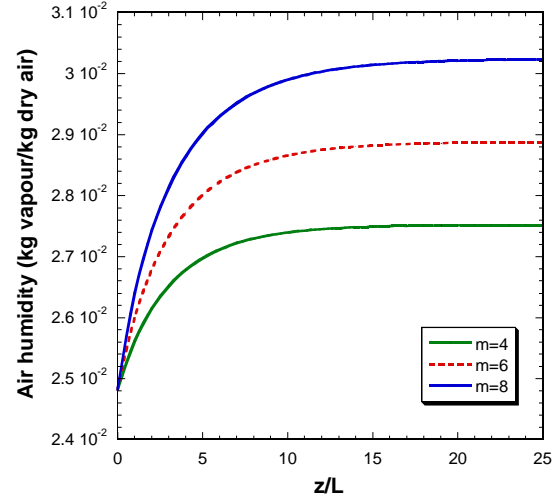


Figure 8: Gas humidity along the dryer for three values of  $m$ .

#### 4. CONCLUDING REMARKS

A model for the semi-continuous food drying process in a tunnel is developed in this work after being calibrated with experimental results for a particular product (i.e. to find  $D_0$ ). This model can be efficiently used for the design and optimization of the continuous drier system for tomatoes employed in N. Erasmio using low-temperature geothermal waters.

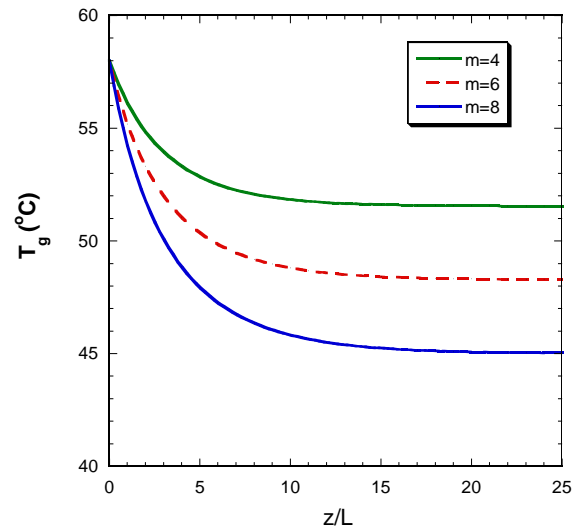
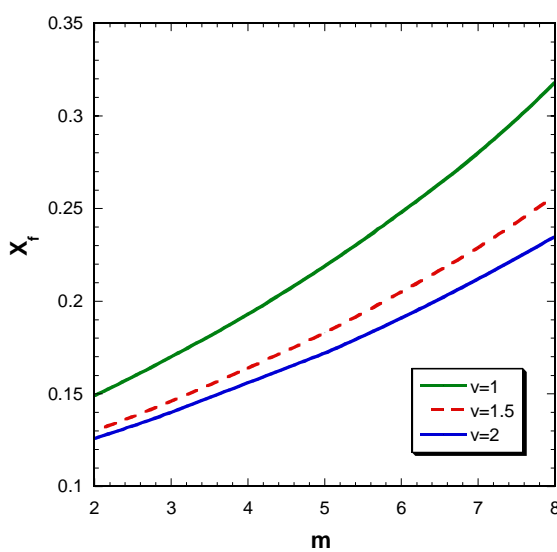


Figure 9: Gas temperature along the dryer for three values of  $m$ .



**Figure 10: Moisture of the final product as a function of air velocity  $u$  (in m/s).**

## REFERENCES

Andritsos, N., Dalampakis, P., and Kolios, N.: Use of Geothermal Energy for Tomato Drying, *GeoHeat Center Quarterly Bul.*, **24**(1), (March 2003) 9-13.

Datta, A.K. Porous media approaches to studying simultaneous heat and mass transfer in food processes. I: Problem formulations. *J. Food Engineering*, **80** (2007) 80-95.

Fellows, P.J.: Food Processing Technology: Principles and Practice, CRC Press, New York, pp. 311-339 (2000).

Glueckauf, E. and Coates, J.I.: Theory of chromatography, Part 4. The influence of incomplete equilibrium on the front boundary of chromatograms and the effectiveness of separation, *J. Chem. Soc.* (1947) 1315-1321.

Hawlader, M.N.A., Uddin, M.S., Ho, J.S., and Teng, A.B.W.: Drying Characteristics of Tomatoes, *J. Food Engineering*, **14**, (1991) 259-268.

Keey, R.B.: Drying, Principle and Practice, Pergamon Press, New York, 1972.

Kiranoudis, C.T., Maroulis, Z.B., Tsami, E., and Marinos-Kouris, D.: Equilibrium Moisture Content and Heat of Desorption of Some Vegetables, *J. Food Engineering*, **20**, (1993) 55-74.

Kocaebe, D., Younsi, R., Poncsak, S., Kocaebe, Y.: Comparison of different models for the high temperature heat treatment of wood, *Int. J. Thermal Sciences*, **46** (2007) 707-716.

Krokida, M.K., Karathanos, V.T., Maroulis, Z.B., and Marinos-Kouris, D.: Drying Kinetics of Some Vegetables, *J. Food Engineering*, **59**, (2003) 391-403.

Luikov, A.V.: Systems of Differential Equations of Heat and Mass Transfer in Capillary-porous Bodies, *Int. J. Heat Mass Transfer*, **18**, (1975) 1-14.

Lund, J.W., Freeston, D.H., Boyd, T.L.: Direct application of Geothermal Energy: 2005 Worldwide Review, *Geothermics*, **34**, (2005) 691-727.

Mujumdar, A.S.: Handbook of Industrial Drying, Marcel Dekker Inc., New York, pp. 137-145 (1987).

Togrul, H.: Simple modeling of infrared drying of fresh apple slices, *J. Food Engineering*, **71** (2005) 311-323.

Vallous, N.A., Gavrielidou, M.A., Karapantsios, T.D. and Kostoglou, M. Performance of a double drum dryer for producing pregelatinized maize starches, *J. Food Engineering*, **51**, 171-183, 2002.

Yotis, A., Tsimpanogiannis, I.N., Stubos, A.K., Yortsos, Y.C.: Pore network study of the characteristic periods in the drying of porous materials, *J. Colloid Interface Science*, **297** (2006), 738-748.